

Teaching the Principles of Statistical Dynamics

Kingshuk Ghosh and Ken A. Dill

Department of Biophysics, University of California, San Francisco CA 94143

Mandar M. Inamdar, Erosyni Seitaridou, and Rob Phillips^{1y}

Division of Engineering and Applied Science and ¹ Kavli Nanoscience Institute,
California Institute of Technology, Pasadena, CA 91125

We describe a simple framework for teaching the principles that underlie the dynamical laws of transport: Fick's law of diffusion, Fourier's law of heat flow, the Newtonian viscosity law, and mass-action laws of chemical kinetics. In analogy with the way that the maximization of entropy over microstates leads to the Boltzmann law and predictions about equilibria, maximizing a quantity that E. T. Jaynes called "Caliber" over all the possible microtrajectories leads to these dynamical laws. The principle of Maximum Caliber also leads to dynamical distribution functions which characterize the relative probabilities of different microtrajectories. A great source of recent interest in statistical dynamics has resulted from a new generation of single-particle and single-molecule experiments which make it possible to observe dynamics one trajectory at a time.

PACS numbers: 51.10.+d 05.40.-a 05.70.Ln

I. INTRODUCTION

We describe an approach for teaching the principles that underlie the dynamical laws of transport: of particles (Fick's law of diffusion), energy (Fourier's law of heat flow), momentum (the Newtonian law for viscosity),¹ and mass-action laws of chemical kinetics.² Recent experimental advances now allow for studies of forces and flows at the single-molecule and nanoscale level, representative examples of which may be found in the references.^{3,4,5,6,7,8,9,10} For example, single-molecule methods have explored the packing of DNA inside viruses,⁷ and the stretching of DNA and RNA molecules.^{9,10} Similarly, video microscopy now allows for the analysis of trajectories of individual submicron size colloidal particles¹¹, and the measurement of single-channel currents has enabled the kinetic studies of DNA translocation through nanopores.^{3,6}

One of the next frontiers in biology is to understand the "small numbers" problem: how does a biological cell function, given that most of its proteins and nucleotide polymers are present in numbers much smaller than Avogadro's number?¹² For example, one of the most important molecules, a cell's DNA, occurs in only a single copy. Also, it is the flow of matter and energy through cells that makes it possible for organisms to maintain a relatively stable form.¹³ Hence, in order to function, cells always have to be in this state far from equilibrium. Thus, many problems of current interest involve small systems that are out of equilibrium. Our interest here is two-fold: to teach our students a physical foundation for the phenomenological macroscopic laws, which describe the properties of averaged forces and flows, and to teach them about the dynamical fluctuations, away from those average values, for systems containing small numbers of particles.

In this article, we describe a very simple way to teach these principles. We start from the "principle of Maximum Caliber", first described by E. T. Jaynes.¹⁴ It aims to provide the same type of foundation for dynamics of many-degree-of-freedom systems that the second law of thermodynamics provides for equilibria of such systems. To illustrate the principle, we use a slight variant of one of the oldest and simplest models in statistical mechanics, the Dog-Flea Model, or Two-Urns Model.^{15,16} Courses in dynamics often introduce Fick's law, Fourier's law, and the Newtonian fluid-mechanics phenomenological laws, rather than deriving them from some deeper foundation. Here, instead, we describe a simple unified perspective that we have found useful for teaching these laws from a foundation in statistical dynamics. In analogy with the role of microstates as a basis for the properties of equilibria, we focus on microtrajectories as the basis for predicting dynamics. One argument that might be leveled against the kind of framework presented here is that in the cases considered here, it is not clear that it leads to anything different from what one obtains using conventional nonequilibrium thinking. On the other hand, often, restating the same physical result in different language can provide a better starting point for subsequent reasoning. This point was well articulated by Feynman in his Nobel lecture¹⁷ who noted: "Theories of the known, which are described by different physical ideas may be equivalent in all their predictions and are hence scientifically indistinguishable. However, they are not psychologically identical when trying to move from that base into the unknown. For different views suggest different kinds of modifications which might be made and hence are not equivalent in the hypotheses one generates from them in one's attempt to understand what is not yet understood."

We begin with the main principle embodied in Fick's Law. Why do particles and molecules in solution flow from

regions of high concentration toward regions of low concentration? To keep it simple, we consider one-dimensional diffusion along a coordinate x . This is described by Fick's first law of particle transport,^{1,2} which says that the average flux $\langle hJ \rangle$, is given in terms of the gradient of average concentration, $\langle hc \rangle = \langle c \rangle$, by

$$\langle hJ \rangle = -D \frac{\partial \langle hc \rangle}{\partial x} \quad (1)$$

where D is the diffusion coefficient. In order to clearly distinguish quantities that are dynamical averages from those that are not, we indicate the averaged quantities explicitly by brackets, $\langle \cdot \rangle$. We describe the nature of this averaging below, and the nature of the dynamical distribution functions over which the averages are taken. But first, we briefly review the standard derivation of the diffusion equation. Combining Fick's first law with particle conservation,

$$\frac{\partial \langle hc \rangle}{\partial t} = - \frac{\partial \langle hJ \rangle}{\partial x}; \quad (2)$$

gives Fick's second law, also known as the diffusion equation:

$$\frac{\partial \langle hc \rangle}{\partial t} = D \frac{\partial^2 \langle hc \rangle}{\partial x^2}; \quad (3)$$

Solving Eq. (3) subject to two boundary conditions and one initial condition gives both $\langle hc(x;t) \rangle$, the average concentration in time and space, and the average flux $\langle hJ(x;t) \rangle$, when no other forces are present. The generalization to situations involving additional applied forces is the Smoluchowski equation.²

A simple experiment shows the distinction between averaged quantities vs. individual microscopic realizations. Using a microfluidic chip like that shown in Fig. (1a), it is possible to create a small fluid chamber divided into two regions by control valves. The chamber is filled on one side with a solution containing a small concentration of micron-scale colloidal particles. The other region contains just water. The three control valves on top of that microfluidic chamber serve two purposes: The two outer ones are used for isolation so that no particles can diffuse in and out of the chamber, while the middle control valve provides the partition between the two regions. The time evolution of the system is then monitored after the removal of the partition (see Fig. (1b)). The time-dependent particle density is determined by dividing the chamber into a number of equal-sized boxes along the long direction and by computing histograms of the numbers of particles in each slice as a function of time. This is a colloidal solution analog of the gas diffusion experiments of classical thermodynamics. The corresponding theoretical model usually used is the diffusion equation. Fig. (1c) shows the solution to the diffusion equation, as a function of time, for the geometry of the microfluidic chip. The initial condition is a step function in concentration at $x = 200 \text{ m}$ at time $t = 0$.

We use this simple experiment to illustrate one main point. The key distinction is that the theoretical curves are very smooth, while there are very large fluctuations in the experimentally observed dynamics of the particle densities. The fluctuations are large because the number of colloidal particles is small, tens to hundreds. The experimental data shows that the particle concentration $c(x;t)$ is a highly fluctuating quantity. It is not well described by the standard smoothed curves that are calculated from the diffusion equation. Of course, when averaged over many trajectories or when particles are at high concentrations, the experimental data should approach the smoothed curves that are predicted by the classical diffusion equation. Our aim here is to derive Fick's Law and other phenomenological transport relations at a microscopic level, so that we can consider both the behaviors of average properties and the fluctuations, i.e., the dynamical distribution functions, and to illustrate the Maximum Caliber approach.

II. THE EQUILIBRIUM PRINCIPLE OF MAXIMUM ENTROPY

We are interested here in dynamics, not statics. However, our strategy follows so closely the Jaynes derivation of the Boltzmann distribution law of equilibrium statistical mechanics,^{2,18} that we first show the equilibrium treatment. To derive the Boltzmann law, we start with a set of equilibrium microstates $i = 1; 2; 3; \dots; N$ that are relevant to the problem at hand. We aim to compute the probabilities p_i of those microstates in equilibrium. We define the entropy, S , of the system as

$$S(\{p_i\}) = -k_B \sum_{i=1}^N p_i \ln p_i; \quad (4)$$

where k_B is the Boltzmann constant. The equilibrium probabilities, $p_i = p_i$ are those values of p_i that cause the entropy to be maximal, subject to two constraints:

$$\sum_{i=1}^N p_i = 1; \quad (5)$$

which is a normalization condition that insures that the probabilities p_i 's sum to one, and

$$\langle E \rangle = \sum_i p_i E_i; \quad (6)$$

which says that the energies, when averaged over all the microstates, sum to the macroscopically observable average energy.

Using Lagrange multipliers α and β to enforce the first and second constraints, respectively, leads to an expression for the values p_i that maximize the entropy:

$$\sum_i [1 - \ln p_i - \beta E_i] = 0; \quad (7)$$

The result is that

$$p_i = \frac{e^{-\beta E_i}}{Z}; \quad (8)$$

where Z is the partition function, defined by

$$Z = \sum_i e^{-\beta E_i}; \quad (9)$$

After a few thermodynamic arguments, the Lagrange multiplier β can be shown to be equal to $1/k_B T$.¹⁸ This derivation, first given in this simple form by Jaynes,¹⁸ identifies the probabilities that are both consistent with the observable average energy and that otherwise maximize the entropy. Jaynes justified this strategy on the grounds that it would be the best prediction that an observer could make, given the observable, if the observer is ignorant of all else. In this case, the observable is the average energy. While this derivation of the Boltzmann law is now quite popular, its interpretation as a method of prediction, rather than as a method of physics, is controversial. Nevertheless, for our purposes here, it does not matter whether we regard this as a description of physical systems or as a strategy for making predictions.

Now, we switch from equilibrium to dynamics, but we use a similar strategy. We switch from the Principle of Maximum Entropy to what Jaynes called the Principle of Maximum Caliber.¹⁴ In particular, rather than focusing on the probability distribution $p(E_i)$ for the various microstates, we seek $p[f_i(t)g]$, where $f_i(t)$ is the i^{th} microscopic trajectory of the system. A gain we maximize an entropy-like quantity, obtained from $p[f_i(t)g]$, to obtain the predicted distribution of microtrajectories. If there are no constraints, this maximization results in the prediction that all the possible microtrajectories are equally likely during the dynamical process. In contrast, certain microtrajectories will be favored if there are dynamical constraints, such as may be specified in terms of the average flux.

In the following section, we use the Maximum Caliber strategy to derive Fick's Law using the Dog-Flea model, which is one of the simplest models that contain the physics of interest.

III. FICK'S LAW FROM THE DOG-FLEA MODEL

We want to determine the diffusive time evolution of particles in a one-dimensional system. The key features of this system are revealed by considering two columns of particles separated by a plane, as shown in Fig. (2). The left-hand column (1) has $N_1(t)$ particles at time t and the right-hand column (2) has $N_2(t)$ particles. This is a simple variant of the famous "Dog-Flea" model of the Ehrenfest's introduced in 1907.^{15,16} Column (1) corresponds to Dog (1), which has N_1 fleas on its back at time t , and column (2) corresponds to Dog (2), which has N_2 fleas at time t . In any time interval between time t and $t + \Delta t$, any flea can either stay on its current dog, or it can jump to the other dog. This model has been used extensively to study the Boltzmann H-theorem and to understand how the time asymmetry of diffusion processes arises from an underlying time symmetry in the laws of motion.^{15,16,19} Our model is used for a slightly different purpose. In particular, our aim is to take a well-characterized problem like diffusion and to reveal how the Principle of Maximum Caliber may be used in a concrete way. We follow the conventional definition of flux,

of a number of particles transferred per unit time, and per unit area. For simplicity, we take the cross-sectional area to be unity.

First, consider the equilibrium state of our Dog-Flea model. The total number of ways of partitioning the $(N_1 + N_2)$ fleas (particles) is $W(N_1; N_2)$,

$$W(N_1; N_2) = \frac{(N_1 + N_2)!}{N_1! N_2!} \quad (10)$$

The state of equilibrium is that for which the entropy, $S = k_B \ln W$ is maximal. A simple calculation shows that the entropy is maximal when the value $N_1 = N_1$ is as nearly equal to $N_2 = N_2$ as possible. In short, at equilibrium, both dogs will have approximately the same number of fleas, in the absence of any bias.

Our focus here is on the dynamics (on how the system reaches that state of equilibrium). We discretize time into a series of intervals τ . We define a dynamical quantity p , which is the probability that a particle (flea) jumps from one column (dog) to the other in any time interval τ . Thus, the probability that a flea stays on its dog during that time interval is $q = 1 - p$. We assume that p is independent of time t , and that all the fleas and jumps are independent of each other.

In equilibrium statistical mechanics, the focus is on the microstates. However, for dynamics we focus on processes, which, at the microscopic level, we call the microtrajectory. Characterizing the dynamics requires more than just information about the microstates; we must also consider the processes. Let m_1 represent the number of particles that jump from column (1) to (2), and m_2 is the number of particles that jump from column (2) to (1), between time t and $t + \tau$. There are many possible different values of m_1 and m_2 : it is possible that no fleas will jump during the interval τ , or that all the fleas will jump, or that the number of fleas jumping will be in between those limits. Each one of these different situations corresponds to a distinct microtrajectory of the system in this idealized dynamical model. We need a principle to tell us what number of fleas will jump during the time interval τ at time t . Because the dynamics of this model is so simple, the implementation of the caliber idea is reduced to nothing more than a simple exercise in enumeration and counting using the binomial distribution.

A. The Dynamical Principle of Maximum Caliber

The probability, $W_d(m_1; m_2 | N_1; N_2)$, that m_1 particles jump to the right and that m_2 particles jump to the left in a discrete unit of time τ , given that there are $N_1(t)$ and $N_2(t)$ fleas on the dogs at time t is

$$W_d(m_1; m_2 | N_1(t); N_2(t)) = \underbrace{p^{m_1} q^{N_1 - m_1} \frac{N_1!}{m_1! (N_1 - m_1)!}}_{W_{d_1}} \underbrace{p^{m_2} q^{N_2 - m_2} \frac{N_2!}{m_2! (N_2 - m_2)!}}_{W_{d_2}} \quad (11)$$

W_d is a count of microtrajectories in dynamics problems in the same vein that W counts microstates for equilibrium problems. In the same spirit that the Second Law of Thermodynamics says to maximize W to predict states of equilibrium, now for dynamics, we maximize W_d over all the possible microtrajectories (i.e. over m_1 and m_2) to predict the fluxes of fleas between the dogs. This is the implementation of the Principle of Maximum Caliber within this simple model. Maximizing W_d over all the possible processes (different values of m_1 and m_2) gives our prediction (right flux $m_1 = m_1$ and left flux $m_2 = m_2$) for the macroscopic flux that we should observe in experiments.

Since the jumps of the fleas from each dog are independent, we find our predicted macroscopic dynamics by maximizing W_{d_1} and W_{d_2} separately, or for convenience their logarithms:

$$\frac{\partial \ln W_{d_i}}{\partial m_i} \bigg|_{N_i, m_i = m_i} = 0; \quad i = 1; 2 \quad (12)$$

Note that applying Stirling's approximation to Eq. (11) W_d gives:

$$\ln W_{d_i} = m_i \ln p + (N_i - m_i) \ln q + N_i \ln N_i - m_i \ln m_i - (N_i - m_i) \ln (N_i - m_i) \quad (13)$$

We call $C = \ln W_d$ the caliber. Maximizing C with respect to m gives

$$\frac{\partial \ln W_{d_i}}{\partial m_i} = \ln p - \ln q - \ln m_i + \ln (N_i - m_i) = 0 \quad (14)$$

This result may be simplified to yield

$$\ln \frac{m_i}{N_i} = \ln \frac{p}{1-p}; \quad (15)$$

which implies that the most probable jump number is simply given by

$$m_i = pN_i; \quad (16)$$

But since our probability distribution W_d is nearly symmetric about the most probable value of ux , the average number and the most probable number are approximately the same. Hence, the average net flux to the right will be,

$$hJ(t)_i = \frac{m_1 - m_2}{t} = p \frac{N_1(t) - N_2(t)}{t} = \frac{p x^2}{t} \frac{c(x;t)}{x}$$

which is Fick's law, in this simple model, and where the diffusion constant is given by $D = p x^2 = t$. We have rewritten $N_1 - N_2 = c x$.

Hence we have a simple explanation for why there is a net flux of particles diffusing across a plane down a concentration gradient: more microscopic trajectories lead downhill than uphill. It shows that the diffusion constant D is a measure of the jump rate p . This simple model does not make any assumptions that the system is "near-equilibrium", i.e., utilizing the Boltzmann distribution law, for example, and thus it indicates that Fick's Law ought also to apply far from equilibrium. For example, we could have imagined that for very steep gradients, Fick's Law might have been only an approximation and that diffusion is more accurately represented as a series expansion of higher derivatives of the gradient. But, at least within the present model, Fick's Law is a general result which emerges from counting up microtrajectories. On the other hand, we would expect Fick's law to break down when the particle density becomes so high that the particles start interacting with each other thus spoiling the assumption of independent particle jumps.

B. Fluctuations in Diffusion

Above, we have shown that the most probable number of leaps that jump from dog (1) to dog (2) between time t and $t + \Delta t$ is $m_1 = pN_1(t)$. The model also tells us that sometimes we will have fewer leaps jumping during that time interval, and sometimes we will have more leaps. These variations are a reflection of the fluctuations resulting from the system following different microscopic pathways.

We focus now on predicting the fluctuations. To illustrate, let us first make up a table of W_d , the different numbers of possible microtrajectories, taken over all the values of m_1 and m_2 (Table (I)). To keep this illustration simple, let us consider the following particular case: $N_1(t) = 4$ and $N_2(t) = 2$. Let us also assume $p = q = 1/2$. Here, then, are the multiplicities of all the possible routes of leap. A given entry tells how many microtrajectories correspond to the given choice of m_1 and m_2 .

Notice first that the table confirms our previous discussion. The dynamical process for which W_d is maximal (12 microtrajectories, in this case), occurs when $m_1 = pN_1 = 1/2 \cdot 4 = 2$, and $m_2 = pN_2 = 1/2 \cdot 2 = 1$. You can compute the probability of that particular flux by dividing $W_d = 12$ by the sum of entries in this table, which is $2^6 = 64$ the total number of microtrajectories. The result, which is the fraction of all the possible microtrajectories that have $m_1 = 2$ and $m_2 = 1$, is 0.18. We have chosen an example in which the particle numbers are very small, so the fluctuations are large; they account for more than 80 percent of the flow. In systems having large numbers of particles, the relative fluctuations are much smaller than this.

Now look at the top right corner of this table. This entry says that there is a probability of $1/64$ that both leaps on dog (2) will jump to the left while no leaps will jump to the right, implying that the net flux, for that microtrajectory, is actually backwards, relative to the concentration gradient. We call these "bad actor" microtrajectories. In those cases, particles flow to increase the concentration gradient, not decrease it. Traditionally, "Maxwell's Demon" was an imaginary microscopic being that was invoked in similar situations in heat flow processes, i.e., where heat would flow from a colder object to heat up a hotter one, albeit with low probability.²⁰ In particular, the Demon was supposed to capture the bad actor microtrajectories. At time t , there are 4 leaps on the left dog, and 2 on the right. At the next instant in time, $t + \Delta t$, all 6 leaps are on the left dog, and no leaps are on the right-hand dog. Notice that this is not a violation of the Second Law, which is a tendency towards maximum entropy, because the Second Law is only a statement that the average flow must increase the entropy; it says nothing about the fluctuations.

Similarly, if you look at the bottom left corner of the table, you see a regime of "super flux": a net flux of 4 particles to the right, whereas Fick's Law predicts a net flow of only 2 particles to the right. This table illustrates that Fick's Law is only a description of the average or most probable flow, and it shows that Fick's Law is not always exactly

correct at the microscopic level. However, such violations of Fick's Law are of low probability, a point that we will make more quantitative below. Such fluctuations have been experimentally measured in small systems.²¹

We can further elaborate on the fluctuations by defining the "potencies" of the microtrajectories. We define the potency to be the fraction of all the trajectories that lead to a substantial change in the macrostate. The potencies of trajectories depend upon how far the system is from equilibrium. To see this, let us continue with our simple system having 6 particles. The total number of microscopic trajectories available to this system at each instant in our discrete time picture is $2^6 = 64$. Suppose that at $t = 0$ all 6 of these particles are in dog (1). The total number of microscopic trajectories available to the system can be classified once again using m_1 and m_2 , where in this case $m_2 = 0$ since there are no dogs on dog (2) (See Table. (II)).

What fraction of all microtrajectories changes the occupancies of both dogs by more than some threshold value, say $N_i > 1$? In this case, we find that 57 of the 64 microtrajectories cause a change greater than this to the current state. We call these potent trajectories.

Now, let us look at the potencies of the same system of 6 particles in a different situation, $N_1 = N_2 = 3$ when the system is in macroscopic equilibrium (see Table. (III)). Here, only the trajectories with $(m_1; m_2)$ pairs given by $(0;2); (0;3); (1;3); (2;0); (3;0)$, and $(3;1)$ satisfy our criterion. Summing over all of these outcomes shows that just 14 of the 64 trajectories are potent in this case.

There are two key observations conveyed by these arguments. First, for a system far from equilibrium, the vast majority of trajectories at that time are potent, and move the system significantly away from its current macrostate. Second, when the system is near equilibrium, the vast majority of microtrajectories leave the macrostate unchanged. Let us now generalize from the tables above, to see when fluctuations will be important.

1. Fluctuations and Potencies

A simple way to characterize the magnitude of the fluctuations is to look at the width of the W_d distribution.² It is shown in standard statistics texts that for a binomial distribution such as ours, for which the mean and most probable value both equal $m_i = N p_i$, the variance is $\sigma_i^2 = N_i p_i q_i$. The variance characterizes the width. Moreover, if N_i is sufficiently large, a binomial distribution can be well-approximated by a Gaussian distribution

$$P(m_i; N_i) = \frac{1}{\sqrt{2\pi N_i p_i q_i}} \exp \left[-\frac{(m_i - N_i p_i)^2}{2 N_i p_i q_i} \right]; \quad (17)$$

an approximation we find convenient since it leads to simple analytic results. However, this distribution function is not quite the one we want. We are interested in the distribution of flux, $P(J) = P(m_1 - m_2)$, not the distribution of right-jumps m_1 or left-jumps m_2 alone, $P(m_i)$.

However, due to a remarkable property of the Gaussian distribution, it is simple to compute the quantity we want. If you have two Gaussian distributions, one with mean $\langle x_1 \rangle$ and variance σ_1^2 , and the other with mean $\langle x_2 \rangle$ and variance σ_2^2 , then the distribution function, $P(x_1 - x_2)$ for the difference will also be a Gaussian distribution, having mean $\langle x_1 \rangle - \langle x_2 \rangle$ and variance $\sigma^2 = \sigma_1^2 + \sigma_2^2$.

For our binomial distributions, the means are $m_1 = pN_1$ and $m_2 = pN_2$ and the variances are $\sigma_1^2 = N_1 p q$ and $\sigma_2^2 = N_2 p q$, so the distribution of the net flux, $J = m_1 - m_2$ is

$$P(J) = \frac{1}{\sqrt{2(pqN)}} \exp \left[-\frac{(J - p(N_1 - N_2))^2}{2pqN} \right]; \quad (18)$$

where $N = N_1 + N_2$.

Figure (3) shows an example of the distributions of fluxes at different times, using $p = 0.1$, and starting from $N_1 = 100; N_2 = 0$. We update each time step using an averaging scheme, $N_1(t + \Delta t) = N_1(t) - N_1(t)p + N_2(t)p$. The figure shows how the mean flux is large at first and decays towards equilibrium, $J = 0$. This result could also have been predicted from the diffusion equation. However, equally interesting are the wings of the distributions, which show the deviations from the average flux, and these are not predictable from the diffusion equation. One measure of the importance of the fluctuations in a given dynamical problem is the ratio of the standard deviation, σ , to the mean,

$$\frac{\sigma}{J} = \frac{\sqrt{N pq}}{(N_1 - N_2)p}; \quad (19)$$

In the limit of large N_1 , the above reduces to,

$$\frac{\sigma}{J} = \frac{\sqrt{N pq}}{(N_1 - N_2)p} \approx N^{-1/2}; \quad (20)$$

In a typical bulk experiment, particle numbers are large, of the order of Avogadro's number 10^{23} . In such cases, the width of the flux distribution is exceedingly small and it becomes overwhelmingly probable that the mean flux will be governed by Fick's law. However, within biological cells and in applications involving small numbers of particles, the variance of the flux can become significant. It has been observed that both rotary and translational single motor proteins sometimes transiently step backwards, relative to their main direction of motion.²²

As a measure of the fluctuations, we now calculate the variance in the flux. It follows from Eq. (18) that $\langle J^2 \rangle = Npq$, where $N = N_1 + N_2$. Thus, we can represent the magnitude of the fluctuations as

$$= \frac{\langle J^2 \rangle}{\langle J \rangle^2} = \frac{Npq}{f^2 N^2} = \frac{1}{f} \frac{q}{p} \frac{1}{N};$$

where the quantity $N = N_1 + N_2$ is the total number of sites and $f = (N_1 - N_2)/N$, the normalized concentration difference. The quantity $\frac{1}{f}$ is also a measure of the degree of back flux. In the limit of large N , $\frac{1}{f}$ goes to zero. That is, the noise diminishes with system size. However, even when N is large, $\frac{1}{f}$ can still be large (indicating the possibility of back flux) if the concentration gradient, $N_1 - N_2$, is small.

Let us look now at our other measure of fluctuations, the potency. Trajectories that are not potent should have $\langle j_1 - j_2 \rangle = 0$ which corresponds to a negligible change in the current state of the system as a result of a given microtrajectory. In Fig. (4), the impotent microtrajectories are shown as the shaded band for which $j_1 - j_2 < h$. To quantify this, we define impotent trajectories as those for which $\langle j_1 - j_2 \rangle < h$, ($h = N$). In the Gaussian model, the fraction of impotent trajectories is

$$\text{impotent} = \int_{-h}^h dJ \frac{1}{\sqrt{2Npq}} \exp \left[-\frac{(J - (N_1 - N_2)p)^2}{2Npq} \right] \quad (21)$$

$$= \frac{1}{2} \left[\text{erf} \frac{h + (N_1 - N_2)p}{\sqrt{2Npq}} + \text{erf} \frac{h - (N_1 - N_2)p}{\sqrt{2Npq}} \right]; \quad (22)$$

and corresponds to summing over the subset of trajectories that have a small flux. To keep it simple, we did a computation, taking $p = q = 1/2$, and for which the expression for the probability distribution for the microscopic flux $j_1 - j_2$ is given by Eq. (18). The choice of h is arbitrary, so let us just choose h to be one standard deviation, $h = \sqrt{2Npq}$. Fig. (5) shows potencies for various values of N_1 and N_2 . When the concentration gradient is large, most trajectories are potent, leading to a statistically significant change of the macrostate, whereas when the concentration gradient is small, most trajectories have little effect on the macrostate.

As another measure of fluctuations, let us now consider the "bad actors" (see Fig. (6)). If the average flux is in the direction from dog (1) to dog (2), what is the probability you will observe flux in the opposite direction (bad actors)? Using Eq. (18) for $P(J)$, we get

$$\text{badactors} = \int_{-1}^0 dJ \frac{1}{\sqrt{2Npq}} \exp \left[-\frac{(J - (N_1 - N_2)p)^2}{2Npq} \right] \quad (23)$$

$$= \frac{1}{2} \left[1 - \text{erf} \frac{(N_1 - N_2)p}{\sqrt{2Npq}} \right]; \quad N_2 > N_1 \quad (24)$$

which amounts to summing up the fraction of trajectories for which $J < 0$. Figure (7) shows the fraction of bad actors for $p = q = 1/2$. Bad actors are rare when the concentration gradient is large, and highest when the gradient is small. The discontinuity in the slope of the curve in Fig. (7) at $N_1 = N_2 = 0.5$ is a reflection of the fact that the mean flux abruptly changes sign at that value.

IV. FOURIER'S LAW OF HEAT FLOW

While particle flow is driven by concentration gradients, according to Fick's law, $\langle J \rangle = -D \frac{\partial c}{\partial x}$, energy flow is driven by temperature gradients, according to Fourier's law¹:

$$\langle J_q \rangle = -\kappa \frac{\partial T}{\partial x};$$

Here, J_q is the energy transferred per unit time and per unit cross-sectional area by heat flow and $\partial T / \partial x$ is the temperature gradient that drives it, indicated here for the one-dimensional case. κ , the thermal conductivity,¹ plays the role that the diffusion coefficient plays in Fick's Law.

To explore Fourier's law, we return to the Dog-Flea model as described in Sec. III. Now, columns (1) and (2) can differ not only in their particle numbers, $N_1(t)$ and $N_2(t)$, but also in their temperatures, $T_1(t)$ and $T_2(t)$. To keep it simple here, we assume that each column is at thermal equilibrium and that each particle that jumps carries with it the average energy, $\frac{1}{2}m\bar{v}^2 = k_B T$ from the column it left. Within this simple model, all energy is transported by hot or cold molecules switching dogs. Although in general, heat can also flow by other mechanisms mediated by collisions, for example, our aim here is just the simplest illustration of principle. The average heat flow at time t is

$$h_{q,i} = \frac{m_1}{t} (k_B T_1) - \frac{m_2}{t} (k_B T_2) = \frac{pk_B}{t} [N_1 T_1 - N_2 T_2] \quad (25)$$

where m_1 and m_2 are, as defined in Sec. IIIA the numbers of particles jumping from each column at time t . If the particle numbers are identical, $N_2 = N_1 = N$, then

$$h_{q,i} = \frac{pk_B N}{t} (T_1 - T_2) = \frac{T}{x};$$

which is Fourier's Law for the average heat flux, within this two-column model. The model predicts that the thermal conductivity is $\kappa = (pk_B N x) / t$, which can be expressed in a more canonical form as $\kappa = \rho k_B n v_{av} l$, when written in terms of the particle density $n = N/x$ and the average velocity, $v_{av} = x/t$. Our simple model gives the same thermal conductivity as given by the kinetic theory of gases,¹ $\kappa = (1/2)k_B n v_{av} l$, where l is the mean free path, if px in our model corresponds to $l/2$, half the mean-free path. Hence, this simple model captures the main physical features of heat flow, again by appealing to the idea of summing over the weighted microtrajectories available to the system.

V. NEWTONIAN VISCOSITY

Another phenomenological law of gradient-driven transport is that of Newtonian viscosities,¹

$$\tau = \eta \frac{dv_y}{dx};$$

where τ is the shear stress that is applied to a fluid, dv_y/dx is the resultant shear rate, and the proportionality coefficient, η , is the viscosity of a Newtonian fluid. Whereas Fick's law describes particle transport and Fourier's law describes energy transport, this Newtonian law describes the transport (in the x -direction, from the top moving plate toward the bottom fixed plate) of linear momentum that acts in the y -direction (parallel to the plates) (see Fig. (8)). Returning to the Dog-Flea model of Sec. III, suppose each particle in column (1) carries momentum $m v_{y1}$ along the y -axis, and that m_1 particles hop from column (1) to (2) at time t , carrying with them some linear momentum. As before, we consider the simplest model that every particle carries the same average momentum from the column it leaves to its destination column.

The flux, J_p , is the amount of y -axis momentum that is transported from one plane to the next in the x -direction, per unit area:

$$h_{p,i} = \frac{m_1}{t} (m v_{y1}) - \frac{m_2}{t} (m v_{y2}) = \frac{pm}{t} [N_1 v_{y1} - N_2 v_{y2}];$$

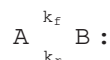
If the number of particles is the same in both columns, $N_2 = N_1 = N$, this simplifies to

$$h_{p,i} = \frac{pm N}{t} [v_{y1} - v_{y2}] = \frac{v_y}{x};$$

which is the Newtonian law of viscosity in this two-column model. The viscosity is predicted by this model to be $\eta = (pm N x) / t$. Converting this to a more canonical form gives $\eta = \rho m n v_{av} l$, where $n = N/x$ is the particle density, and $v_{av} = x/t$ is the average velocity. This is equivalent to the value given by the kinetic theory of gases,¹ $\eta = (1/3) m n l v_{av}$, if px from our model equals $(1/3)l$, one-third of the mean-free path length. Note that this simple model based upon molecular motions will clearly not be applicable to complex fluids where the underlying molecules possess internal structure.

VI. CHEMICAL KINETICS WITHIN THE DOG-FLEA MODEL

Let us now look at chemical reactions using the Dog-Flea model. Chemical kinetics can be modeled using the Dog-Flea model when the fleas have preference for one dog over the other. Consider the reaction



The time-dependent average concentrations, $[A](t)$ and $[B](t)$ are often described by chemical rate equations,²

$$\begin{aligned} \frac{d[A]}{dt} &= -k_f[A] + k_r[B] \\ \frac{d[B]}{dt} &= k_f[A] - k_r[B] \end{aligned} \quad (26)$$

where k_f is the average conversion rate of an A to a B, and k_r is the average conversion rate of a B to an A. These rate expressions describe only average rates; they do not tell us the distribution of rates. Some A's will convert to B's faster than the average rate $k_f[A]$ predicts, and some will convert more slowly. Again, we use the Dog-Flea model as a microscopic model for this process. We use it to consider both the average concentrations and the fluctuations in concentrations.

Now, dog (1) represents chemical species A and dog (2) represents chemical species B. The net chemical flux from 1 to 2 is given by $J_c = m_1 - m_2$. What is different about our model for these chemical processes than in our previous situations is that now the intrinsic jump rate from column 1 (species A), p_1 , is different than the jump rate from column 2, p_2 . This simply reflects the fact that a forward rate can differ from a backward rate in a chemical reaction. Now, fleas have a different escape rate from each dog. Fleas escape from Dog (1) at rate p_1 and fleas escape from Dog (2) at rate p_2 . Maximizing W_d gives $m_1 = N_1 p_1$ and $m_2 = N_2 p_2$, so the average flux (which is the almost the same as the most probable flux because of the approximately symmetric nature of the binomial distribution) at time t is,

$$\langle J \rangle = N_1 p_1 - N_2 p_2 = k_f [A] - k_r [B];$$

which is just the standard mass-action rate law, expressed in terms of the mean concentrations. The mean values satisfy detailed balance at equilibrium ($\langle J \rangle = 0$) $N_2 p_2 = N_1 p_1 = k_f = k_r$.

More interesting than the well-known behavior of the mean chemical reaction rate is the fluctuational behavior. For example, if the number of particles is small, then even when $k_f [A] - k_r [B] > 0$, indicating an average conversion of A's to B's, the reverse can happen occasionally instead. When will these fluctuations be large? As in Sec. III, we first determine the probability distribution of the flux J . In this case, the probability distribution becomes:

$$P(J) = \frac{1}{2^{(p_1 q_1 N_1 + p_2 q_2 N_2)}} \exp \left[-\frac{J (N_1 p_1 - N_2 p_2)}{2 (p_1 q_1 N_1 + p_2 q_2 N_2)} \right]; \quad (27)$$

Again, let us use this flux distribution function to consider the fluctuations in the chemical reaction. The relative variance in the flux is

$$\frac{\langle J^2 \rangle - \langle J \rangle^2}{\langle J \rangle^2} = \frac{p_1 q_1 N_1 + p_2 q_2 N_2}{N_1 p_1 - N_2 p_2};$$

As before, the main message is that when the system is not yet at equilibrium (i.e., the denominator is non-zero), macroscopically large systems will have negligibly small fluctuations. The relative magnitude of fluctuations scales approximately as $N^{-1/2}$. Let us also look at the potencies of microtrajectories as another window into fluctuations. Using Eq. (22) with p_1 and p_2 gives the fraction of trajectories that are in potent as

$$\text{in potent} = \frac{Z_h}{Z} = \frac{\int_h dJ \frac{1}{2^{(p_1 q_1 N_1 + p_2 q_2 N_2)}} \exp \left[-\frac{J (N_1 p_1 - N_2 p_2)}{2 (p_1 q_1 N_1 + p_2 q_2 N_2)} \right]}{\int_{-\infty}^{\infty} dJ \frac{1}{2^{(p_1 q_1 N_1 + p_2 q_2 N_2)}} \exp \left[-\frac{J (N_1 p_1 - N_2 p_2)}{2 (p_1 q_1 N_1 + p_2 q_2 N_2)} \right]} \quad (28)$$

$$= \frac{1}{2} \operatorname{erf} \left[\frac{h + (N_1 p_1 - N_2 p_2)}{2 (p_1 q_1 N_1 + p_2 q_2 N_2)} \right] + \operatorname{erf} \left[\frac{h - (N_1 p_1 - N_2 p_2)}{2 (p_1 q_1 N_1 + p_2 q_2 N_2)} \right]; \quad (29)$$

Using $N_1 + N_2 = N = 100$, and $p_1 = 0.1$ and $p_2 = 0.2$, $\text{in potent} = 1 - \text{in potent}$ as a function of $N_1 = N$ is shown in Fig. 9.

VII. DERIVING THE DYNAMICAL DISTRIBUTION FUNCTION FROM MAXIMUM CALIBER

Throughout this paper, we have used the binomial distribution function, W_d , as the basis for our treatment of stochastic dynamics. The Maximum Caliber idea says that if we find the value of W_d that is maximal with respect to the microscopic trajectories, this will give the macroscopically observable flux. Here, we now restate this in a more general way, and in terms of the probabilities of the trajectories.

Let $P(i)$ be the probability of a microtrajectory i during the interval from time t to $t + \Delta t$. A microtrajectory is a specific set of fleas that jump; for example microtrajectory $i = 27$ might be the situation in which fleas number 4, 8, and 23 jump from dog (1) to (2). We take as a constraint the average number of jumps, $\langle m_i \rangle$, the macroscopic observable. The quantity $\langle m_i \rangle = 3$ in this case indicates that trajectory i involves 3 fleas jumping. We express the caliber C as

$$C = \sum_i \lambda P(i) \ln P(i) - \sum_i \mu_i P(i) + \sum_i \nu P(i) \quad (30)$$

where, λ is the Lagrange multiplier that enforces the constraint of the average flux and μ_i is the Lagrange multiplier that enforces the normalization condition that the $P(i)$'s sum to one. Maximizing the caliber gives the populations of the microtrajectories,

$$P(i) = \exp(-\lambda - \mu_i) \quad (31)$$

Note that the probability $P(i)$ of the i^{th} trajectory depends only on the total number m_i of the jumping fleas. Also, all trajectories with the same m_i have same probabilities. Now, in the same way that it is sometimes useful in equilibrium statistical mechanics to switch from microstates to energy levels, we now express the population $P(i)$ of a given microtrajectory, instead, in terms of $g(m)$ the fraction of all the microtrajectories that involve m jumps during this time interval,

$$g(m) = \sum_i P(i) \delta(m - m_i) \quad (32)$$

where, $g(m) = \frac{1}{N} \sum_i \delta(m - m_i)$ is the "density of trajectories" with flux m (in analogy with the density of states for equilibrium systems), and $Q(m)$ is the probability $P(i)$ of the microtrajectory i with $m_i = m$. In other words, i denotes a microtrajectory (specific set of fleas jumping) while m denotes a microprocess (the number of fleas jumping). The total number of i 's associated with a given m is precisely $g(m)$. It can also be easily seen that,

$$\sum_i P(i) = \sum_{m=0}^N g(m) Q(m) = \sum_{m=0}^N g(m) = 1 \quad (33)$$

$$\langle m_i \rangle = \sum_i m_i P(i) = \sum_{m=0}^N m g(m) Q(m) = \sum_{m=0}^N m g(m) \quad (34)$$

Thus, the distribution of jump-processes written in terms of the jump number, m , is

$$g(m) = \frac{N!}{m!(N-m)!} \exp(-\lambda) \exp(-\mu) \quad (35)$$

The Lagrange multiplier λ can be eliminated by summing over all trajectories and requiring that $\sum_{m=0}^N g(m) = 1$, i.e.,

$$\exp(-\lambda) = \sum_m g(m) e^{-\mu} = \sum_m \frac{N!}{m!(N-m)!} e^{-\mu} = (1 + e^{-\mu})^N \quad (36)$$

Combining Eqs. (35) and (36) gives

$$g(m) = \frac{N!}{m!(N-m)!} \frac{\exp(-\mu)}{(1 + \exp(-\mu))^N} \quad (37)$$

If we now let

$$P = \frac{\exp(-\mu)}{1 + \exp(-\mu)} \quad (38)$$

then we get

$$p^m = \frac{\exp(-\beta \epsilon_m)}{(1 + \exp(-\beta \epsilon_m))^m}; \quad (39)$$

and

$$(1 - p)^{N - m} = \frac{1}{(1 + \exp(-\beta \epsilon_m))^{N - m}}; \quad (40)$$

Combining Eqs. (37), (39), and (40) gives the simple form

$$p(m) = \frac{N!}{m!(N - m)!} p^m (1 - p)^{(N - m)};$$

that we have used throughout this paper in Eq. (11).

V III. S U M M A R Y A N D C O M M E N T S

We have shown how to derive the phenomenological laws of nonequilibrium transport, including Fick's law of diffusion, the Fourier law of heat conduction, the Newtonian law of viscosity, and mass-action laws of chemical kinetics, from a simple physical foundation that can be readily taught in elementary courses. We use the Drog-Fleam model, originated by the Ehrenfests, for describing how particles, energy, or momentum can be transported across a plane. We combine that model with the Principle of Maximum Caliber, a dynamical analog of the way the Principle of Maximum Entropy is used to derive the laws of equilibrium. In particular, according to Maximum Entropy, you maximize the entropy $S(p_1; p_2; \dots; p_N)$ with respect to the probabilities p_i of $N - m$ microstates, subject to constraints, such as the requirement that the average energy is known. That gives the Boltzmann distribution law. Here, for dynamics, we focus on microtrajectories, rather than microstates, and we maximize a dynamical entropy-like quantity, subject to an average flux constraint. In this way, maximizing the caliber is the dynamical equivalent of minimizing a free energy for predicting equilibria. A particular value of this approach is that it also gives us fluctuation information, not just averages. In diffusion, for example, sometimes the flux can be a little higher or lower than the average value expected from Fick's Law. These fluctuations can be particularly important for biology and nanotechnology, where the numbers of particles can be very small, and therefore where there can be significant fluctuations in rates, around the average.

A c k n o w l e d g m e n t s

It is a pleasure to acknowledge the helpful comments and discussions with Dave Dabold, Mike Geller, Jane Kondev, Stefan Muller, Hong Qian, Darren Segall, Pierre Sens, Jim Sethna, Ron Siegel, Andrew Spakowitz, Zhen-Gang Wang, and Paul Wiggins. We would also like to thank Sarina Bromberg for the help with the figures. KAD and MM would like to acknowledge support from NIH grant number R01 GM 034993. RP acknowledges support from NSF grant number CMS-0301657, the Kock foundation, NSF NIRT grant number CMS-0404031, and NIH Director's Pioneer Award grant number DP1 OD 000217.

Electronic address: dill@m axwellucsf.edu

^y Electronic address: phillips@ pboc.caltech.edu

¹ F. Reif, Fundamentals of statistical and thermal physics (McGraw-Hill, NY, 1965).

² K. Dill and S. Bromberg, Molecular driving forces: statistical thermodynamics in chemistry and biology (Garland Science, New York, 2003).

³ J. Kasianowicz, E. Brandin, D. Branton, and D. Deamer, Proc. Nat. Acad. Sci. USA 93, 13770 (1996).

⁴ H. P. Lu, L. Xun, and X. S. Xie, Science 282, 1887 (1998).

⁵ M. Reif, R. S. Rock, A. D. M. Ehta, M. S. Mooseker, R. E. Cheney, and J. A. Spudich, Proc. Nat. Acad. Sci. 97, 9482 (2000).

⁶ A. M. Eller, L. Nivon, and D. Branton, Phys. Rev. Lett. 86, 3435 (2001).

⁷ D. E. Smith, S. J. Tans, S. B. Smith, S. Grimes, D. L. Anderson, and C. Bustamante, Nature 413, 748 (2001).

⁸ H. Li, W. A. Linke, A. F. Oberhauser, M. Carrion-Vazquez, J. G. Kravliet, H. Lu, P. Marszalek, and J. M. Fernandez, Nature 418, 998 (2002).

- ⁹ J. Liphardt, S. Dumont, S. B. Smith, I. Tinoco, and C. Bustamante, *Science* 296, 1832 (2002).
- ¹⁰ C. Bustamante, Z. Bryant, and S. B. Smith, *Nature* 421, 423 (2003).
- ¹¹ E. R. Dufresne, D. Altman, and D. G. Grier, *Europhys. Lett.* 53, 264 (2001).
- ¹² B. Alberts, D. Bray, A. Johnson, J. Lewis, M. Raff, K. Roberts, and P. Walter, *Essential Cell Biology: An Introduction to the Molecular Biology of the Cell* (Garland Publishing, New York, 1997).
- ¹³ D. Kondopudi and I. Prigogine, *Modern thermodynamics: From heat engines to dissipative structures* (John Wiley and sons, 1998).
- ¹⁴ E. T. Jaynes, in *E. T. Jaynes: Papers on probability, statistics and statistical physics*, edited by R. D. Rosenkrantz (Kluwer academic publishers, 1980), chap. 14.
- ¹⁵ M. Klein, *Physica* 22, 569 (1956).
- ¹⁶ G. G. Emch and C. Liu, *The logic of thermostatical physics* (Springer-Verlag, NY, 2002).
- ¹⁷ R. P. Feynman, in *Nobel Lectures in Physics: 1901-1995* (World Scientific Publishing Co., 1998).
- ¹⁸ E. T. Jaynes, in *E. T. Jaynes: Papers on probability, statistics and statistical physics*, edited by R. D. Rosenkrantz (Kluwer academic publishers, 1957), chap. 1.
- ¹⁹ M. Kac, *Amer. Math. Monthly* 54, 369 (1947).
- ²⁰ G. Gamow, *One Two Three...Infinity* (Dover Publications, NY, 1988).
- ²¹ G. M. Wang, E. M. Sevick, E. Mittag, D. J. Searles, and D. J. Evans, *Phys. Rev. Lett.* 89, 050601 (2002).
- ²² J. Howard, *Mechanics of motor proteins and the cytoskeleton* (Sinauer Associates Inc., 2001).

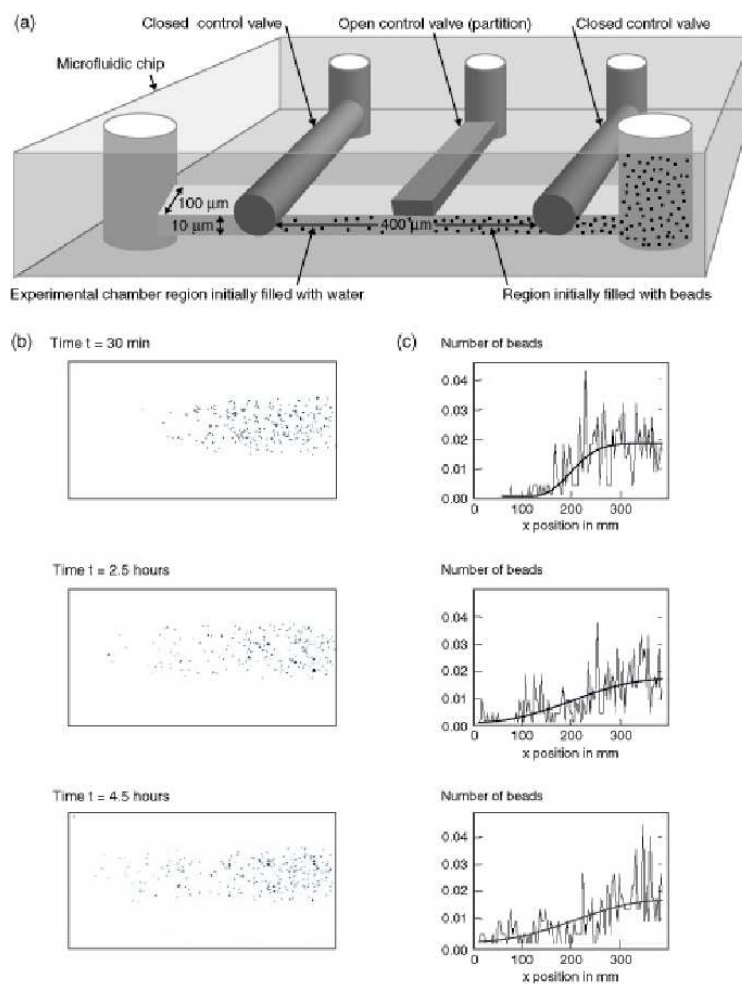


FIG. 1: Colloidal free expansion setup to illustrate diffusion involving small numbers of particles. (a) Schematic of experimental setup (see text for details.) (b) Several snapshots from the experiment. (c) Normalized histogram of particle positions during the experiment. The solution to the diffusion equation for the microfluidic "free expansion" experiment is superposed for comparison.

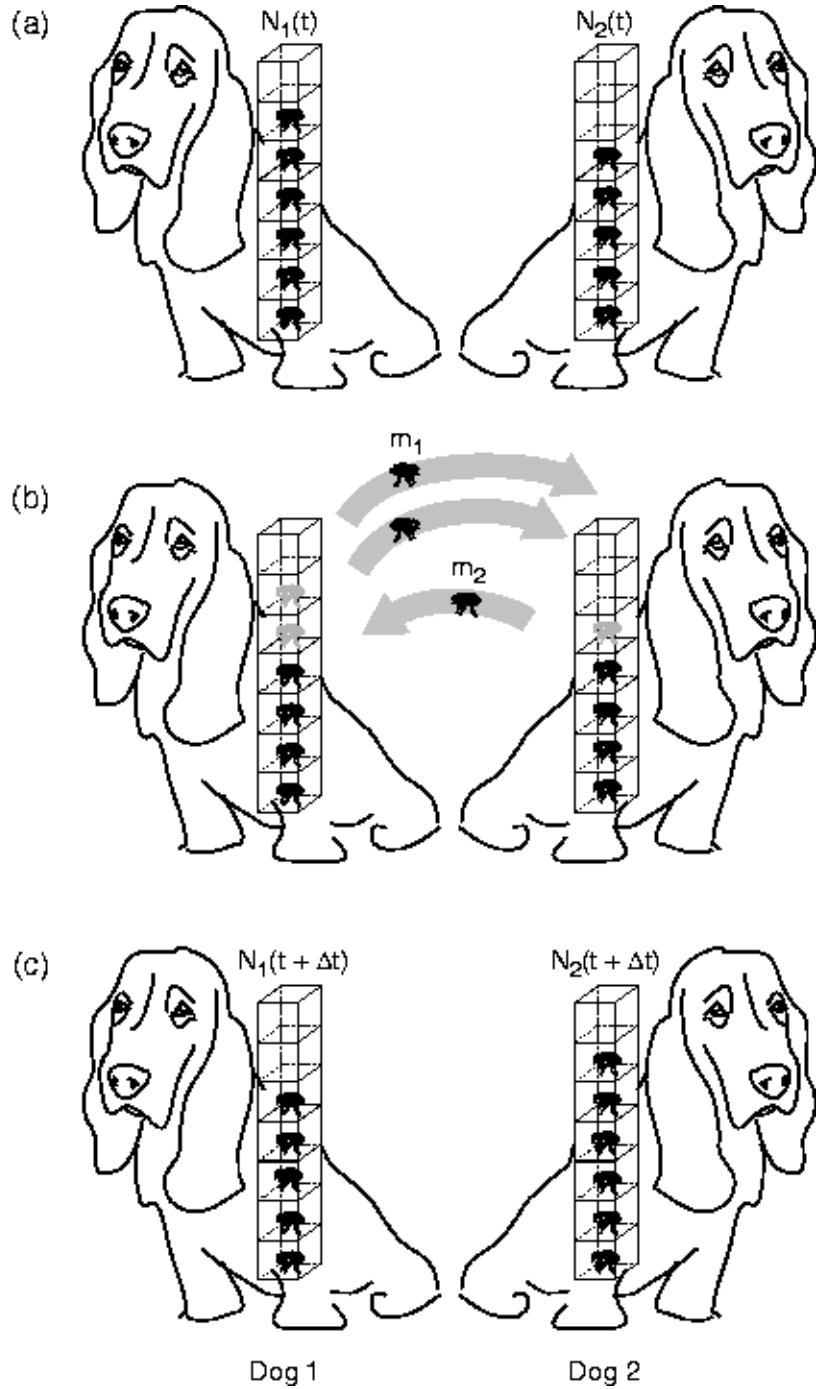


FIG. 2: Schematic of the simple dog-eat-moel model. (a) State of the system at time t , (b) a particular microtrajectory in which two moels jump from the dog on the left and one jumps from the dog on the right, (c) occupancies of the dogs at time $t + \Delta t$.

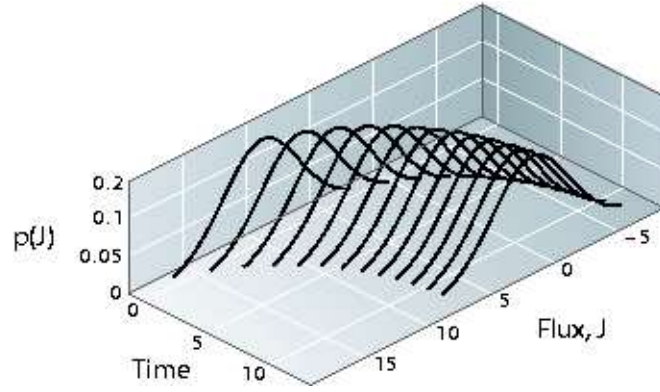


FIG . 3: Schematic of the distribution of fluxes for different time points as the system approaches equilibrium .

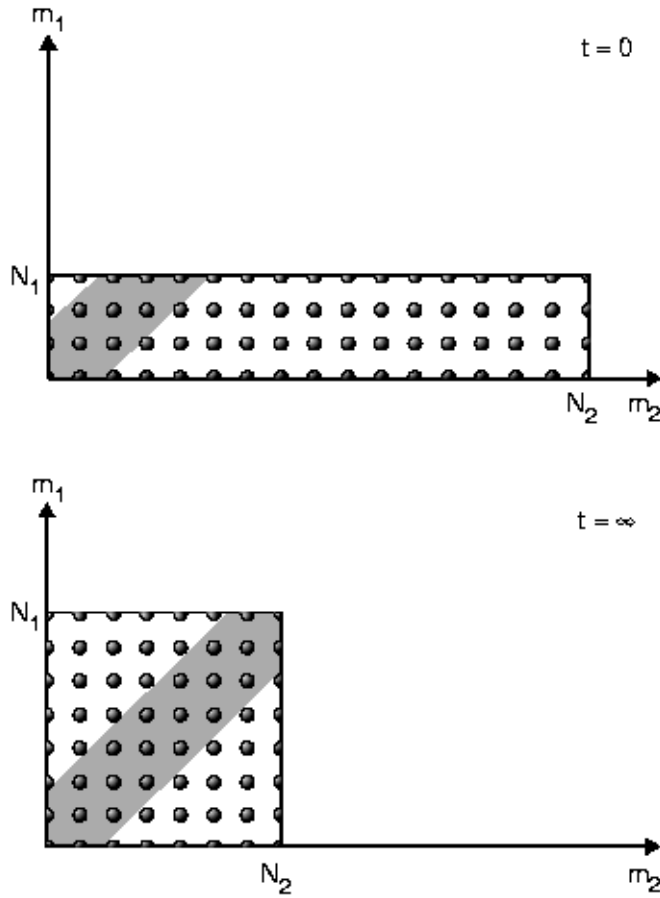


FIG . 4: Schematic of which trajectories are potent and which are in potent. The shaded region corresponds to the in potent trajectories for which m_1 and m_2 are either equal or approximately equal and hence make relatively small change in the macrostate. The unshaded region corresponds to potent trajectories.

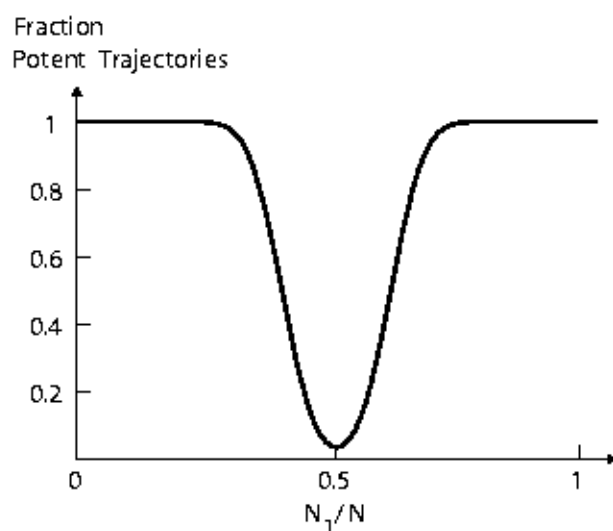


FIG . 5: Illustration of the potency of the microtrajectories associated with different distributions of N particles on the two dogs. The total number of particles $N_1 + N_2 = N = 100$.

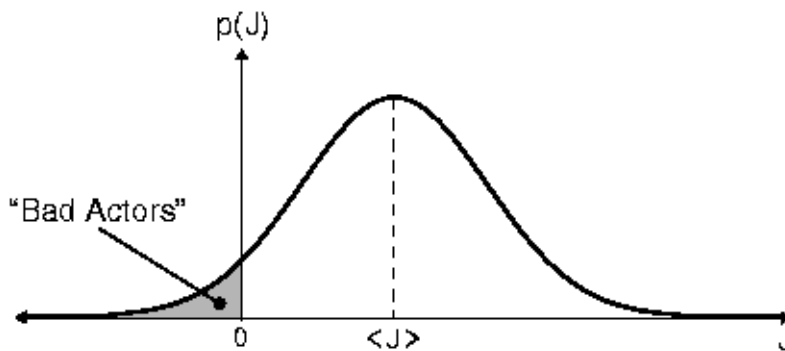


FIG . 6: Illustration of the notion of bad actors. Bad actors are essentially the microtrajectories which contribute net particle motion which has the opposite sign from the macro flux.

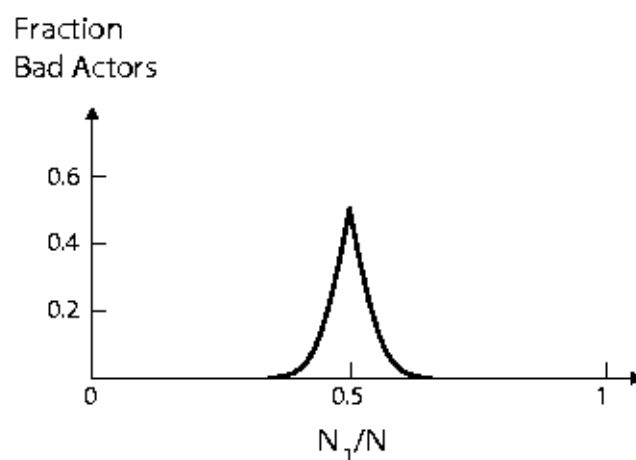


FIG . 7: The fraction of all possible trajectories that go against the direction of the macro ux, for $N = 100$. The fraction of bad actors is highest at $N_1 = N_2 = 50$.

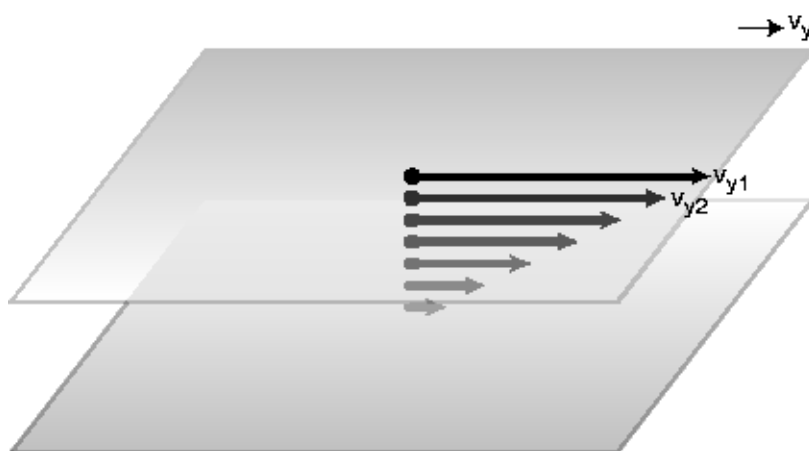


FIG . 8: Illustration of Newton's law of viscosity. The uid is sheared with a constant stress. The uid velocity decreases continuously from its maximum value at the top of the uid to zero at the bottom . There is thus a gradient in the velocity which can be related to the shear stress in the uid.

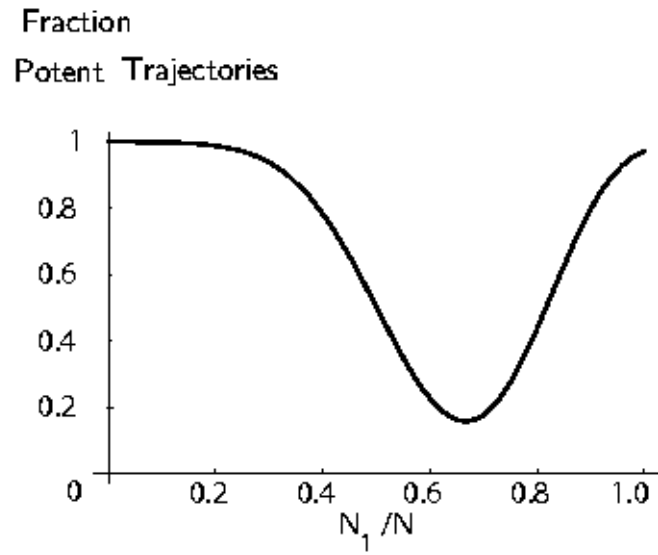


FIG .9: The fraction of potent trajectories, p_{potent} , as a function of N_1/N for $N_1 + N_2 = N = 100$, when $p_1 = 0.1$ and $p_2 = 0.2$ are not equal. The minimum value of potency does not occur at $N_1/N = 0.5$, but at $N_1/N = 0.66$. This value of N_1/N also corresponds to its equilibrium value given by $p_2 = (p_1 + p_2)$.

m_1	m_2	0	1	2
0		1	2	1
1		4	8	4
2		6	12	6
3		4	8	4
4		1	2	1

TABLE I: Trajectory multiplicity table for the specific case where $N_1(t) = 4$ and $N_2(t) = 2$. Each entry in the table corresponds to the total number of trajectories for the particular values of m_1 and m_2 .

m_1	m_2	0
0		1
1		6
2		15
3		20
4		15
5		6
6		1

TABLE II: Trajectory multiplicity table for the specific case $N_1(t) = 6$ and $N_2(t) = 0$ when the system is far from macroscopic equilibrium.

m_1	m_2	0	1	2	3
0		1	3	3	1
1		3	9	9	3
2		3	9	9	3
3		1	3	3	1

TABLE III: Trajectory multiplicity table for the specific case $N_1(t) = 3$ and $N_2(t) = 3$ when the system is at the macroscopic equilibrium.